

Prospects of the Detection of Circumbinary Planets With Kepler and CoRoT Using the Variations of Eclipse Timing

R. Schwarz^{1*}, N. Haghighipour², S. Eggl¹, E. Pilat-Lohinger¹ and B. Funk³

¹*Institute for Astronomy, University of Vienna, A-1180 Vienna, Türkenschanzstrasse 17, Austria*

²*Institute for Astronomy and NASA Astrobiology Institute, University of Hawaii, 2680 Woodlawn Dr., Honolulu, HI, 96822 USA*

³*Department of Astronomy, Eötvös University, H-1117 Budapest, Pázmány Péter setany 1/A, Hungary*

ABSTRACT

In close eclipsing binaries, measurements of the variations in binary’s eclipse timing may be used to infer information about the existence of circumbinary objects. To determine the possibility of the detection of such variations with CoRoT and *Kepler* space telescopes, we have carried out an extensive study of the dynamics of a binary star system with a circumbinary planet, and calculated its eclipse timing variations (ETV) for different values of the mass-ratio and orbital elements of the binary and the perturbing body. Here, we present the results of our study and assess the detectability of the planet by comparing the resulting values of ETVs with the temporal sensitivity of CoRoT and *Kepler*. Results point to extended regions in the parameter-space where the perturbation of a planet may become large enough to create measurable variations in the eclipse timing of the secondary star. Many of these variations point to potentially detectable ETVs and the possible existence of Jovian-type planets.

Key words: methods: numerical, techniques: photometric, binaries: eclipsing, planetary systems, planets: detection

1 INTRODUCTION

Approximately 70 percent of the main and pre-main sequence stars are members of binary or multiple star systems. Observational evidence indicates that many of these systems contain potentially planet-forming circumstellar or circumbinary disks implying that planet formation may be a common phenomenon in and around binary stars (Mathieu 1994; Akeson et al. 1998; Rodriguez et al. 1998; White et al. 1999; Silbert et al. 2000; Mathieu et al. 2000; Trilling et al. 2007).

Many efforts have been made to detect such *binary-planetary* systems. In the past two decade, even though single stars were routinely prioritized in search for extrasolar planets, many of these efforts were successful and resulted in the detection of approximately 40 planet-hosting binary star systems. The discovery of these systems have led to the speculation that many more planets may exist in and around binaries and prompted astronomers to explore the possibility of the detection of these planets with different detection methods. We refer the reader to *Planets in Binary Star Systems* (Haghighipour 2010) for an up to date

and comprehensive review of the current state of observational and theoretical research in this area.

In general, one can distinguish three types of planetary orbits in a binary star system (Fig. 1):

- (i) **S-Type**, where the planet orbits one of the two stars,
- (ii) **P-Type**, where the planet orbits the entire binary,
- (iii) **T-Type**, where the planet orbits close to one of the two equilibrium points L_4 and L_5 (Trojan planets).

Currently, the most known planets in binary systems are in S-type orbits [for more details see e.g., Pilat-Lohinger & Dvorak (2002), Pilat-Lohinger et al. (2003), and Haghighipour et al. (2010)]. The stellar separations of many of these binaries are larger than 100 AU implying that the perturbation of their farther companions on the formation and dynamical evolution of planets around their planet-hosting stars may be negligible. However, in the past few years, radial velocity and Astrometry surveys have been able to identify five binary star systems with separations of approximately 20 AU where one of the stars is host to a Jovian-type planet. These systems, namely, GL 86 (Queloz et al. 2000; Els et al. 2001), γ Cephei (Hatzes et al. 2003), HD 41004 (Zucker et al. 2004; Raghavan et al. 2006), HD 196885 (Correia et al. 2008), and HD 176051 (Mutterspaugh et al. 2010) present unique

* E-mail: schwarz@astro.univie.ac.at

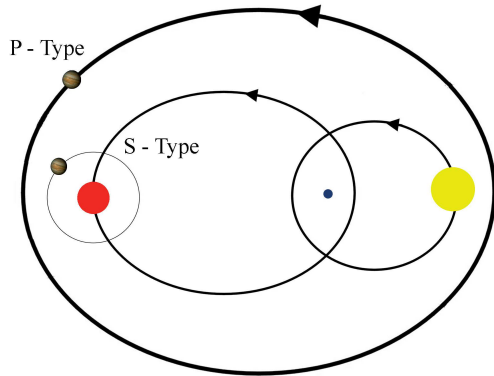


Figure 1. Schematic illustration of S-type and P-type orbits in a binary star system. The yellow and red circles represent the stars of the binary revolving around their common center of mass (the blue circle).

cases for the study of planet formation and dynamics in binaries as the perturbation of their secondary stars will have significant effects on the dynamics of their circumpriary disks and their capability in forming planets.

The success of radial velocity and astrometry in detecting planets in S-type orbits raises the question that whether other techniques can also detect planets in and around binary stars. A recent success has come in the form of the detection of the first P-type planets using the ETV method. Modeling the variations in the eclipse timing of the binary NN Ser, Beuermann et al. (2010) have shown that this system is host to two planets with minimum masses of 2.2 and 6.9 Jupiter-masses in a 2:1 mean-motion resonance in circumbinary orbits.

Our work has been motivated by this discovery. NN Ser (ab) is an eclipsing short period binary which shows long-term ETVs. The detection of P-type planets around this system suggests that close, eclipsing binaries may be promising candidates in the search for new exoplanets. As many of these binaries lie in the discovery space of CoRoT (Goldmann 2010) and *Kepler* (Coughlin et al. 2010) space telescopes, we focus our study on exploring the prospects of the detection of such objects.

The idea of photometric detection of extrasolar planets around eclipsing binaries was first presented by Schneider & Chevreton (1990). This idea that was later developed by many authors (Schneider & Doyle 1995; Doyle et al. 1998; Doyle & Deeg 2004; Deeg et al. 2008; Mutterspaugh et al. 2010), is based on the fact that a circumbinary planet can perturb the orbit of the two stars and create variations in their eclipse timing. The measurements of these variations, when compared with theoretical models, can reveal information about the mass and orbital elements of the perturbing planet.

Recently Sybilsky et al. (2010) studied the potential of the ETV method in detecting giant planets in circular, circumbinary orbits. These authors have shown that ground-based photometry may have advantage over CoRoT and *Kepler* space telescopes in detecting circumbinary planets. They suggest that the selective nature of the target stars in the fields of view of CoRoT and *Kepler* causes the ETV signals of eclipsing binaries in these regions to be smaller than

the detection sensitivities of these telescopes. These authors also suggest that if target binary stars include presumably less stable contact binaries, the CoRoT's and *Kepler*'s capabilities of detecting of circumbinary planets increase by four times.

In this paper, we extend the study by Sybilsky et al. (2010) to binaries with planets in eccentric and resonant orbits. It is expected that similar to the transit timing variation method where TTV signals are strongly enhanced when the transiting and perturbing planets are in resonance (Agol et al. 2005; Agol & Steffen 2007; Steffen & Agol 2005), a resonant perturbing circumbinary planet will also produce high ETV signals. The goal of our study is to identify regions of the parameter-space for which this signal is within the temporal sensitivity of CoRoT and *Kepler* space telescopes.

The outline of our paper is as follows. We present our models in section 2 and discuss their stability in section 3. Section 4 has to do with the calculations of ETVs and the prospects of the detection of P-type planets. Section 5 concludes this study by summarizing the results and discussing their implications.

2 MODEL

We consider a close, eclipsing binary with a giant planet in a P-type orbit. To ensure that the effect of the variations of the mass-ratio of the binary is included in our study, we consider the following three models where m_1 and m_2 are the masses of the primary and secondary stars, respectively,

- **model 1:** $m_1 = m_2 = 0.3 M_{\text{sun}}$,
- **model 2:** $m_1 = 1, m_2 = 0.5 M_{\text{sun}}$,
- **model 3:** $m_1 = m_2 = 1 M_{\text{sun}}$.

As most of the stars in the solar neighborhood are of spectral type M, this choice of models ensures that low-mass binary stars are also included in our simulations.

Eclipsing binaries are morphologically classified as

- (i) **detached systems**, if neither component fills its Roche lobe (separated stars),
- (ii) **semi-detached systems**, if only one component fills its Roche lobe, and
- (iii) **over contact systems**, if both components exceed their Roche lobes.

The Roche lobe marks the volume limit at which the star may begin to lose substantial amount of matter to its companion. In this study we consider a **detached binary** with an initial separation of 0.05 AU. For the binary models 1 and 3, this separation corresponds to a period of approximately 5 and 3 days, respectively. As shown by Goldmann (2010), most candidate eclipsing binaries in the discovery space of CoRoT have periods between 1 and 10 days.

When dealing with close binaries such as the models considered here, the intrinsic eccentricity of the binary (e_{bin}) can be neglected. This is due to the high probability of circularization that is caused by interstellar tidal forces. In this study, we consider the initial orbital eccentricity of the binary to be zero or have very low values. The latter is due to the fact that the timescale of circularization is dependent upon specific stellar parameters (Zahn & Bouchet 1989).

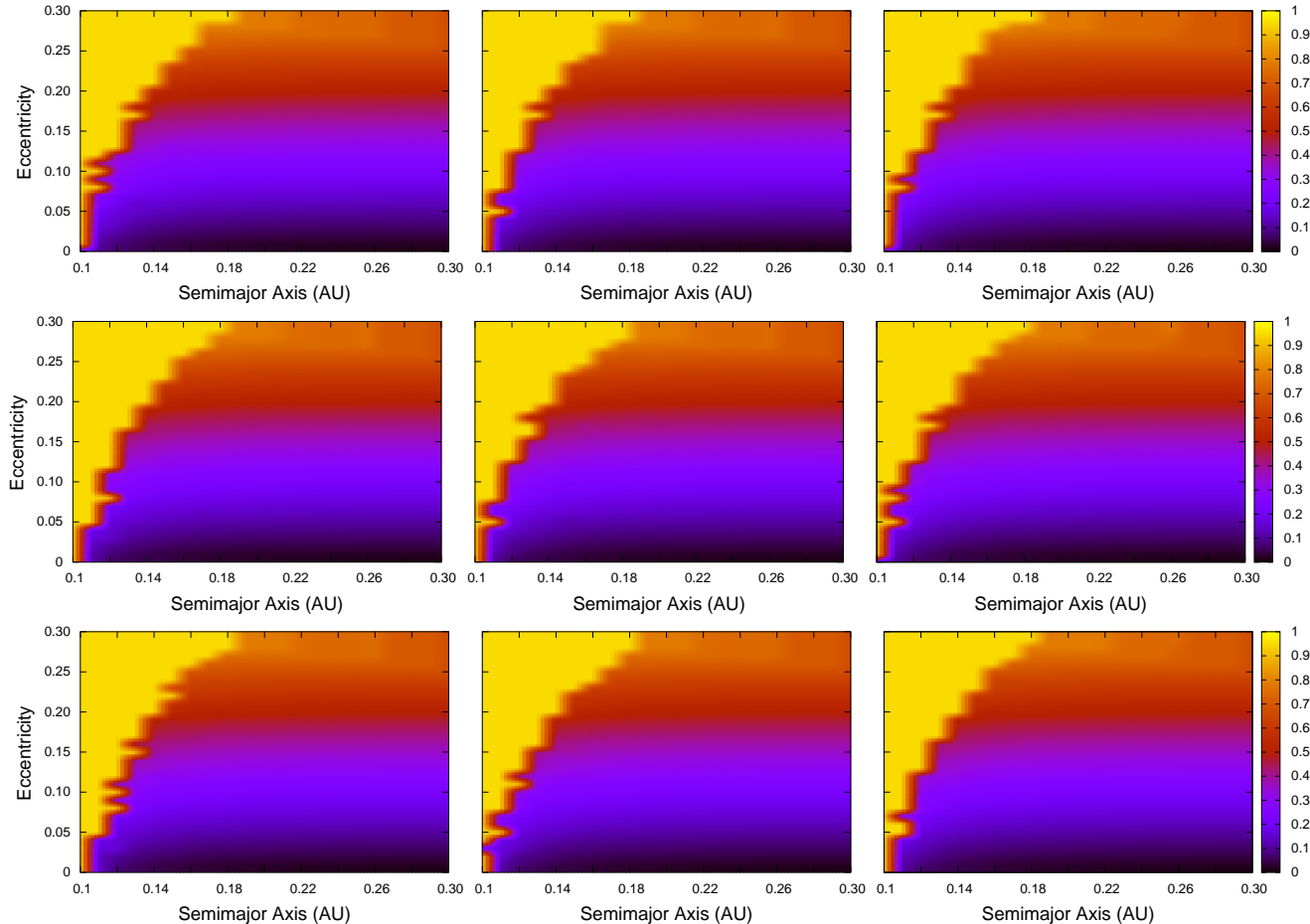


Figure 2. The e_{\max} maps of a circumbinary planet in the binary model 1 (left column), 2 (middle column), and 3 (right column). The top row shows the maps for a $1 M_J$ planet, the middle row is for a $5 M_J$ planet, and the bottom row corresponds to a $10 M_J$ object. The violet and blue regions represent small values of e_{\max} and correspond to bound orbits whereas the yellow region points to escape.

3 STABILITY ANALYSIS

Prior to calculating the variations in the eclipse timing, it is necessary to identify regions where a P-type planet can have a stable orbit. For this purpose, we integrated the Newtonian three-body system of the binary and its planet for different values of the planet’s mass and orbital elements. The mass of the planet was taken to be 1, 5, and 10 Jupiter-masses. The values of its semimajor axis and orbital eccentricity with respect to the barycenter of the system were varied between $a = 0.1 - 0.3$ AU and $e = 0 - 0.3$ in increments of $\Delta a = 0.01$ AU and $\Delta e = 0.01$, respectively.

Numerical integrations were carried out using the Lie-series method and Bulirsch-Stoer integrator (Lichtenegger 1984; Hanslmeier & Dvorak 1985; Eggl & Dvorak 2010). We integrated the system for 10^4 years which corresponds to the following number of periods of the planet at 0.1 AU:

- **model 1:** 2.45×10^5 periods,
- **model 2:** 3.90×10^5 periods,
- **model 3:** 4.50×10^5 periods.

The stability of the planetary motion was controlled by measuring the value of its maximum orbital eccentricity (e_{\max}). We monitored the changes in the eccentricity of the planet throughout the integration and determined its high-

est value. If the orbit of the planet became parabolic ($e = 1$), we considered the system to be unstable.

Figure 2 shows the values of planet’s e_{\max} at different distances from the barycenter of the binary. The left column corresponds to the binary model 1, the middle column to binary model 2, and the right column to binary model 3. Also, from top to bottom, each row corresponds to the values of e_{\max} for a $1 M_J$, $5 M_J$, and $10 M_J$, respectively. In each panel, the axes represent the initial values of the semimajor axis and eccentricity of the planet at the beginning of the integration. The color at each point depicts the maximum value that the eccentricity of the planet acquired during the integration. As indicated by the scale on the right side of the figure, yellow corresponds to parabolic orbits and denotes instability.

An inspection of the e_{\max} maps shown in Fig. 2 indicates that for planets in circular or low eccentricity orbits, the range of the semimajor axis for which the planetary orbit may be bound is large and does not change much for different values of the planet’s mass. For instance, as shown by the top left panel of this figure, the boundary of the unstable zone for a $1 M_J$ planet in a circular orbit in the binary model 1 is interior to 0.1 AU. This suggests that all circular orbits with semimajor axes larger than 0.1 AU in this model may be bound. As the mass of the planet grows

(middle and bottom panels of the left column in Fig. 2), the outer boundary of the unstable region slowly progresses toward larger semimajor axes. Such a trend is also seen in the e_{\max} maps of binary models 2 and 3. As shown by the lower panels in the middle and right columns, the boundary of the unstable zone for circular orbits is slightly shifted outward to 0.11 AU. These results are consistent with the results of the stability analysis of a test particle in a circumbinary orbit as presented by Dvorak et al. (1989) and Holman & Wiegert (1999). According to the estimate of the boundary of the stable zone as given by these authors, the critical distance beyond which the orbit of a Jovian planet in all our three binary models will be stable is in the range of 0.1 to 0.12 AU.

While the value of e_{\max} can be used to identify parabolic (unstable) orbits, it cannot be used as a rigorous indicator of planet's orbital stability. A low value of e_{\max} implies a bound planetary orbit. But that is only for the duration of the integration, and there is no guarantee that the orbit of the planet will stay bound for a long time. In order to determine the orbital stability of the planet, we used the Fast Lyapunov Indicator (FLI) (Froeschlé et al. 1997). The FLI is a chaos indicator that measures the exponential divergence of nearby trajectories and distinguishes between regular and chaotic motion. For details of this technique, we refer the reader to Froeschlé et al. (1997), Lega & Froeschlé (2001) and Fouchard et al. (2002). Applications of FLI to planetary motion in binary star systems can be found in Pilat-Lohinger & Dvorak (2002), Pilat-Lohinger et al. (2003) and Haghighipour et al. (2010).

Figure 3 shows a sample of an FLI stability map for a 1 M_J planet in binary model 1. The colors in this figure represent the values of FLI (the logarithmic scale on the right) which depict the degree of chaos. Dark colors correspond to less chaotic and regular orbits. As shown by this figure, there is a region in the parameter-space where the orbit of the planet is likely stable (dark area between 0.1 and 0.3 AU).

A comparison between the dark region of Fig. 3 and its corresponding region in the system's e_{\max} map in Fig. 2 (upper left panel) points to an interesting observation: even though the maximum values of the planet's orbital eccentricity can reach to high values, the orbit of the planet may still be stable. In other words, elevated planetary eccentricities do not necessarily correspond to instability. For instance, as shown by the upper left panel of Fig. 2, orbits with initial eccentricities of 0.3 may have e_{\max} values up to 0.7. Nevertheless, according to the FLI results shown in Fig. 3, they are probably long-term stable.

Similar comparison can also be made between the chaotic region of Fig. 3 (indicated by red and yellow colors) and the system's e_{\max} map in Fig. 2. The results point to an inverse phenomenon, that is, instability among seemingly bound orbits. For instance, while for semimajor axes ranging from $a = 0.11$ AU to $a = 0.14$ AU, and the eccentricities between $e = 0.05$ and $e = 0.15$, the e_{\max} map suggests bound planetary orbits, the FLI stability map indicates chaotic motion. The different color shades for chaotic orbits in the FLI map have resulted from the fact that the degree of divergence depends on the initial conditions of the orbits. Even though this shading may suggest less chaotic 'islands' in parameter-space, when compared to the corre-

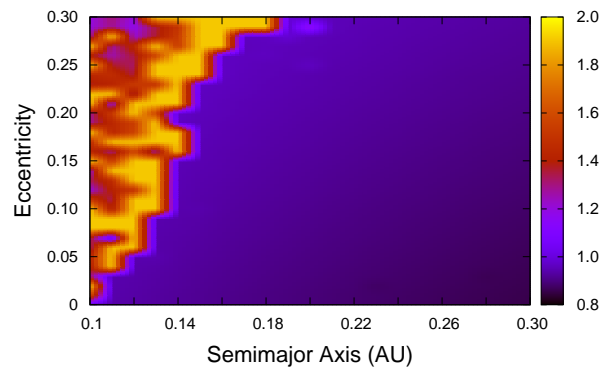


Figure 3. The FLI stability map for a 1 M_J P-type planet in the binary model 1. The violet and blue regions (small values of the FLI) correspond to regions of regular motion, and red and yellow denote chaotic orbits.

sponding e_{\max} map, one can see that orbits inside the chaotic border zone become parabolic.

Using the combination of e_{\max} and FLI analyses, we identified the stable planetary orbits in all our three binary models. As an example, the number of stable circular orbits are shown in Table 1. As expected, stability is almost independent of the mass-ratio of the binary.

We also carried out simulations for non-zero values of the binary's eccentricity. Figure 4 shows the maps of e_{\max} for a 1 M_J planet in the binary model 1. The binary eccentricity was chosen to be $e_{\text{bin}} = 0.05, 0.1$, and 0.15 . Table 2 shows the number of stable orbits for these simulations. As shown here, the unstable region expands out by more than two folds when $e_{\text{bin}} = 0.1$. Our analysis indicated that for the value of the binary eccentricity $e_{\text{bin}} = 0.2$, only 4 orbits remained stable (Table 2).

The results of our stability analysis allow us to focus our calculations of ETVs on the region of the parameter-space where P-type planets have stable orbits. As shown, the planet's stable region shrinks for large values of its eccentricity as well as the eccentricity of the binary. Initial binary eccentricities beyond $e_{\text{bin}} = 0.15$ move this region to large distances ($a = 0.24$ AU) where the perturbing effect of the planet on the dynamics of the binary becomes negligible (Fig. 4). The closest possible stable orbit for a planet ($a = 0.1$ AU) is when the planet is Jupiter-mass, and both the planet and binary have circular orbits. As a result, for the purpose of calculating ETVs, we only consider fully circularized binaries.

4 CALCULATION OF ECLIPSE TIMING VARIATIONS

As indicated by the results of the stability analysis, a Jovian planet in a P-type orbit may be stable in the vicinity of a binary star system. Although small, the gravitational perturbation of this planet may affect the motions of the two stars and cause their orbits to deviate from Keplerian. In an eclipsing binary, these deviations result in variations in the time and duration of the eclipse. Similar to the variations in the transit timing of a planet due to a second perturber (Miralda-Escudé & Adams 2005; Holman & Murray 2005; Agol & Steffen 2007; Kipping 2009a,b; Ford & Holman

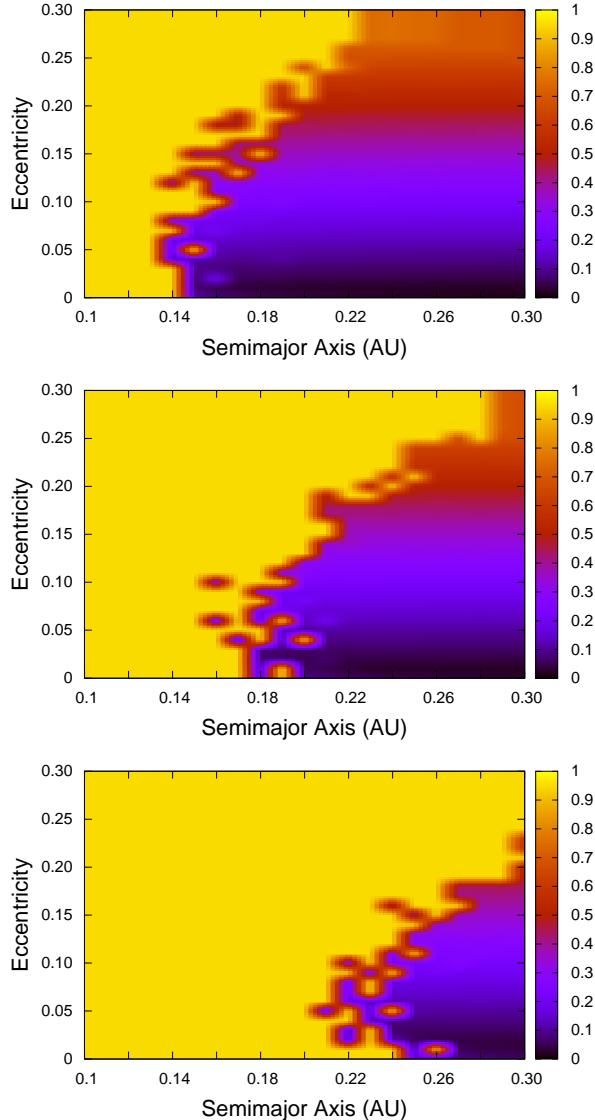


Figure 4. The e_{\max} maps of a $1 M_J$ planet in the binary model 1 with $e_{\text{bin}} = 0.05$ (top), 0.1 (middle), and 0.15 (bottom).

Table 1. Number of stable orbits of all three binary models for $e_{\text{bin}} = 0$.

Model	$M_{\text{planet}} (M_J)$	stable orbits (number)	stable orbits (%)
model 1	1	540	82.9
	5	530	81.4
	10	527	80.9
model 2	1	531	81.5
	5	529	81.2
	10	526	80.7
model 3	1	539	82.6
	5	538	82.6
	10	533	81.8

Table 2. Number of stable orbits for binary model 1 and for different values of e_{bin} .

e_{bin}	$M_{\text{planet}} (M_J)$	stable orbits (numbers)	stable orbits (%)
0.00	1	540	82.9
0.05	1	407	62.5
0.10	1	270	41.4
0.15	1	127	19.5
0.20	1	4	0.6

2007), the variations in eclipse timing can be used to infer information about the mass and orbital elements of the circumbinary planet. In this section, we calculate the eclipse timing variations of our model binary star systems for different values of the mass and orbital parameters of the binary and its P-type planet. Our goal is to identify a range of these parameters for which the magnitude of ETVs will be within the temporal sensitivity of CoRoT and *Kepler* space telescopes.

We simulated the dynamics of our binary models and their P-type planets in a barycentric coordinate system. Simulations were carried out for 1 year corresponding to approximately 70 transits of the secondary star. We calculated ETVs by determining the difference between the eclipse timing (t_1) of the unperturbed system (star-star) and its corresponding value (t_2) in the perturbed case (star-star-planet)¹. Additionally, we subtracted the planetary induced constant rate of apsidal precession. We also Fourier-analyzed the resulting signal and compared the superposition of the main frequencies to simple estimates on maximum amplitudes $[(dt_{\max} - dt_{\min})/2]$ for the entire duration of integration. In cases where the differences between Fourier-composition-derived ETVs and maximum amplitudes were lower than 10%, we chose to present the ETVs' maximum amplitudes.

4.1 Implication for the detection of circumbinary planets

As mentioned earlier, we would like to identify regions of the parameter-space for which the ETV signals of an eclipsing binary will be detectable by CoRoT and *Kepler* space telescopes. Since as indicated by the stability analysis, stable planetary orbits move to large distances as the eccentricity of the binary increases, we limited our calculations to circular systems. We recall that in all our models, the separation of the binary is 0.05 AU.

For the planet's motion, we considered both resonant and non-resonant orbits. Similar to transit timing variation, ETV signals are strongly enhanced when the P-type planet and the binary are in a mean-motion resonance (MMR). Results of our stability analysis indicate that the location of the 2:1 MMR at 0.079 AU is too close to the binary's center of mass to be stable (Dvorak et al. 1989, Holman & Wiegert 1999). We, therefore, considered cases where the planet is in a 3:1 (0.104 AU) and a 4:1 (0.126 AU) MMR.

¹ We chose to integrate the binary two body problem instead of taking analytical solutions in order to minimize the influence of the numerical integration algorithm on the results.

For the non-resonant orbits, we chose the semimajor axis of the planet to have the values of 0.2 AU and 0.3 AU. The eccentricity of the planet's orbit in all cases was chosen to be 0 or 0.15, and its angular variables (inclination, mean-anomaly, longitude of the ascending node, argument of pericenter) were set to zero.

Table 3 shows the results of the calculation of ETVs for a circular binary. Even though MMRs did not have too much influence on the stability of the system, the most prominent ETVs were found at 3:1 and 4:1 resonances. Figure 5 shows these ETVs for a 1 Jupiter-mass planet.

In order to assess the detectability of our ETV signals with CoRoT and *Kepler*, we compared our results with the values of the Detectable Timing Amplitudes (DTA) of these telescopes. As shown by Sybilsky et al. (2010), given the typical photometric error, the value of the DTA for CoRoT is approximately 4 sec for a 12 mag star and 16 sec for a star with 15.5 mag. Similar analysis suggests that stars with magnitudes between 9 and 14.5 mag will have DTAs ranging from 0.5 to 4 sec with *Kepler*.

Figure 6 shows a comparison between the values of DTA calculated by Sybilsky et al. (2010) and the amplitudes of ETVs obtained from our simulations. The x-axes in this figure represent the planet's initial semimajor axis and the y-axes show the maximum amplitude of ETVs. In cases where the value of ETV is larger than 40 sec, this value is indicated on the top of its corresponding bar. As a point of comparison, the maximum values of the DTAs for CoRoT (16 sec for a 15.5 mag star) and *Kepler* (4 sec for a 14.5 mag star) are also shown. When the ETV signal is higher than these observational thresholds, we assume that a planet may be indirectly detectable via eclipse timing of the secondary star.

As shown in this figure, planets in mean-motion resonances present the highest probability of detection. This is expected as these planets create the largest variations in eclipse timing. Also, as indicated by the left column, binary model 1 with low-mass stars present the best prospect for detecting P-type Jovian planets. As the masses of the binary stars increase, the prospect of detection shifts toward larger planets. For instance, in binary model 3 (right column), a 5 Jupiter-mass planet can be detected in orbits smaller than 0.2 AU. As expected, the highest prospect of detection is for a 10 Jupiter-mass object (lower right panel). Figure 6 also shows that while planets in circular orbits produce the largest ETVs when in resonance, slight eccentricity in the orbit of the planet increases the prospect of its detection and extends its detectability to large distances. The latter is more pronounced for larger planets around more massive binaries as in these cases, the planetary orbit stays stable when its orbital eccentricity is slightly increased.

5 DISCUSSION

We have studied the prospects of the detection of circumbinary planets with CoRoT and *Kepler* space telescopes using the variations of binary eclipse timing. The uninterrupted high precision photometry of these telescopes (Koch et al. 2004; Alonso et al. 2008) has given them unique capability for detecting small variations in eclipse timing measurements. We have calculated such variations in several binary models with circumbinary planets and compared the

Table 3. Systems with ETVs that are potentially detectable with CoRoT and *Kepler*.

Model	M_{planet} (M_J)	a (AU)	e	ETV (sec)
model 1	1	0.104	0	316
	1	0.126	0, 0.15	40, 69
	5	0.126	0, 0.15	179, 349
	5	0.2	0, 0.15	25, 51
	5	0.3	0.15	28
	10	0.126	0, 0.15	339, 730
	10	0.2	0, 0.15	46, 97
	10	0.3	0.15	54
model 2	1	0.126	0.15	32
	5	0.126	0, 0.15	55, 161
	10	0.126	0	108
	10	0.2	0, 0.15	17, 21
model 3	1	0.104	0	51
	5	0.126	0, 0.15	31, 59
	10	0.126	0, 0.15	60, 117
	10	0.2	0.15	16

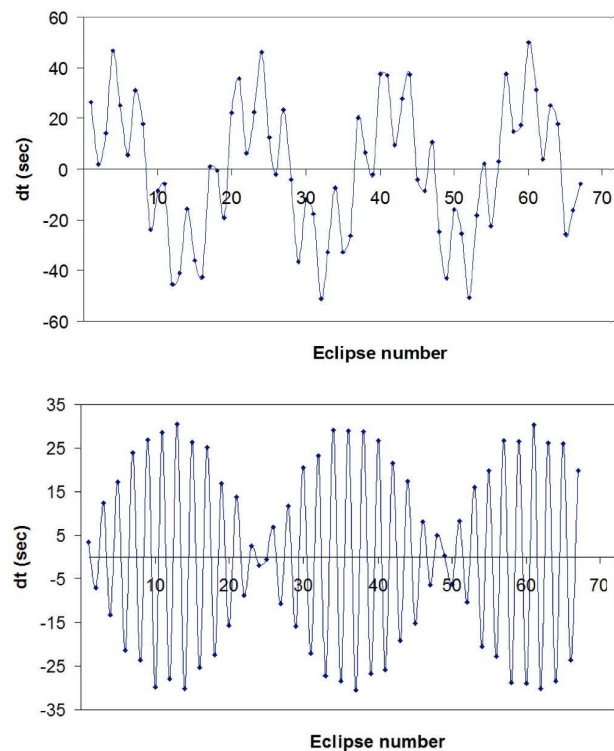


Figure 5. The graphs of ETVs for a 1 M_J planet in a circular orbit in the binary model 3. The planet is in a 3:1 MMR in the top panel and a 4:1 MMR in the bottom one.

results with the temporal sensitivity of these telescopes. As expected, the prospect of detection is higher for planets in resonant orbits as these objects create larger ETVs. This is more pronounced when the stars of the binary have low masses. This result is consistent with the findings by Schneider & Doyle (1995). However, it is important to note that low-mass binaries may be hard to identify.

Our study indicates that around solar-mass binaries,

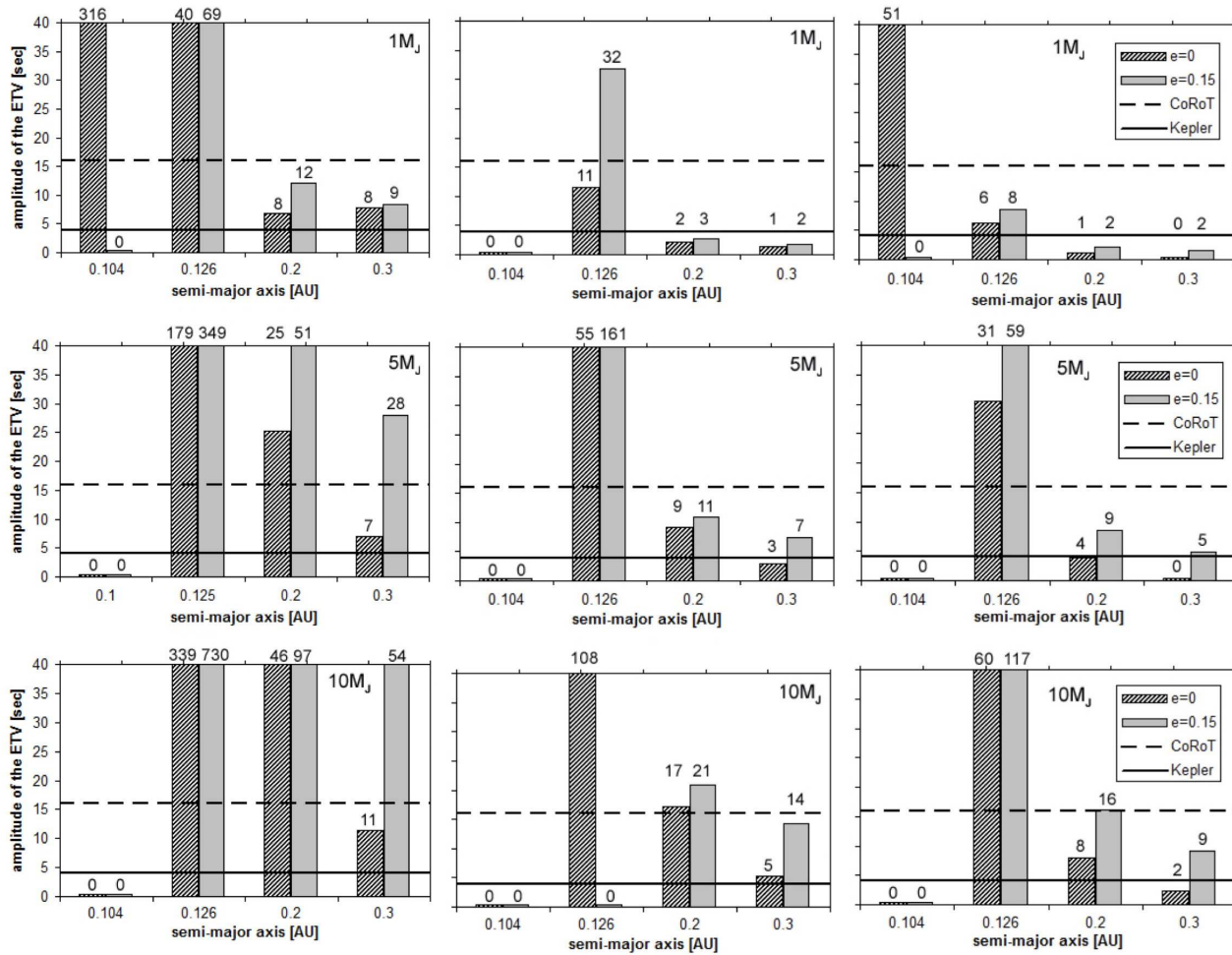


Figure 6. Graphs of the maximum amplitude of ETVs for all three binary models with $e_{\text{bin}} = 0$. The locations of bars on the horizontal axis correspond to 3:1 MMR at 0.104 AU, 4:1 MMR at 0.126 AU, and two non-resonant orbits at 0.2 and 0.3 AU. Graphs are shown for two values of the planet’s orbital eccentricity (0 and 0.15). As a point of comparison, the maximum values of DTAs for CoRoT and *Kepler* (Sybilsky et al. 2010) are also shown.

planets with sizes down to 1 Jupiter-mass can produce detectable signals. In this case, planets have to move in almost circular orbit close ($a \sim 2a_{\text{bin}}$) to binary’s center of mass in order to maintain stability. More massive planets on higher eccentricities may orbit the binary at distances up to approximately $6a_{\text{bin}}$ and still be able to produce ETVs that are detectable by *Kepler*.

Result of our simulations indicate that although the orbital stability of the planet is strongly affected by increasing its eccentricity and the eccentricity of the binary, slight deviations from circular orbits, in particular in the orbit of the planet, result in its periodic close approaches to the binary and creating large ETVs. Our study suggests that when not in a resonance, in general, giant planets on slightly eccentric circumbinary orbits show bigger prospects for having detectable ETVs. With their high precision photometry and long duration of operation, CoRoT and *Kepler* are well suited for indirect planet detection via ETVs, and have the capability of detecting such planets within the durations of their operation.

ACKNOWLEDGMENTS

RS acknowledges supports through the MOEL grant of the ÖFG (Project MOEL 386) and the FWF project P18930. NH acknowledges support from the NASA Astrobiology Institute under Cooperative Agreement NNA04CC08A at the Institute for Astronomy, University of Hawaii, and NASA EXOB grant NNX09AN05G. Supports are also acknowledged through the Austrian FWF Erwin Schrödinger grant no. J2892-N16 for BF, the Austrian FWF project no. P20216 for SE, and the Austrian FWF project no. P22603, P20216 for E. P-L. We thank J. Schneider and G. Wuchterl for fruitful discussions.

REFERENCES

- Agol, E., Steffen, J., Sari, Reém, Clarkson, W. 2005, MNRAS, 359, 567
- Agol, E. & Steffen J.H., 2007, MNRAS, 374, 941.
- Akeson, R. L., Koerner, D. W. & Jensen, E. L. N., 1998, ApJ, 505, 358
- Alonso, R., et al. 2008, A&A, 482, L21

- Beuermann, K. Hessmann, F. V., Dreizler, S., Marsh, T. R., Parsons, S. G., Winget, D. E., Miller, G. F., Schreiber, M. R., Kley, W., Dhillon, V. S., Littlefair, S. P., Copperwheat, C. M., & Hermes, J. J., *A&A*, 521, L60
- Correia, A. C. M., Udry, S., Mayor, M., Eggenberger, A., Naef, D., Beuzit, J.-L., Perrier, C., Queloz, D., Sivan, J.-P., Pepe, F., Santos, N. C., & Ségransan, D. 2008, *A&A*, 479, 271
- Coughlin, J. L., Lopez-Morales, M., Harrison, T. E., Ule, N., Hoffman, D. I., 2010, submitted (arXiv:1007.4295v2)
- Deeg, H. J., Ocana, B., Kozhevnikov, V. P., Charbonneau, D., O'Donovan, F. T., Doyle, L. R. 2008, *A&A*, 480, 563
- Doyle L. R., Deeg H. J., Jenkins J. M., Schneider, J., Ninkov, Z., et al. 1998, Detectability of Jupiter-to-Brown-Dwarf-Mass Companions around Small Eclipsing Binary System, in Rebolo R., Martin, E. L., Zapatero-Osorio M.R. (eds.) *Brown Dwarfs & Extrasolar Planets*. ASP Conference Proc. Vol. 134, 224
- Doyle, L. R., & Deeg, H.-J. 2004, in Norris, R., Stootman, F., eds. *Proceedings of IAU Symposium 213, Bioastronomy 2002: Life Among the Stars*, San Francisco: Astronomical Society of the Pacific, 2003., p.80
- Dvorak, R., Froeschlé, Ch., Froeschlé, C., 1989, *A&A*, 226, 335
- Eggl, S., & Dvorak, R., 2010, *LNP*, 790, 431
- Els, S. G., Sterzik, M. F., Marchis, F., Pantin, E., Endl, M., & Kürster, M. 2001, *A&A*, 370, L1
- Ford, E.B., & Holman, M.J., 2007, *ApJ*, 664, L51
- Fouchard, M., Lega E., Froeschlé Ch., Froeschlé C., 2002, *CeMDA*, 83, 205
- Froeschlé, C., Lega E., Gonzi, R., 1997, *CeMDA*, 67, 41.
- Goldmann, C., *Secular resonances in planetary systems*, Master Thesis, University of Vienna.
- Haghighipour, N., 2010, *Planet in Binary Star Systems* (Berlin: Springer), ISBN: 978-90-481-8686-0
- Haghighipour, N., Dvorak, R., & Pilat-Lohinger, E., 2010, in "Planets in Binary Star Systems", N. Haghighipour (ed.), *Astrophysics and Space Science Library*, Vol. 366. Berlin: Springer, ISBN: 978-90-481-8686-0, p.285-327
- Hanslmeier, A., & Dvorak, R., 1984, *A&A*, 132, 203
- Hatzes, A. P., Cochran, W. D., Endl, M., McArthur, B., Paulson, D.B., Walker, G. A. H., Campbell, B. & Yang, S., 2003, *ApJ*, 599, 1383
- Holman, M. J. & Murray, N. W., 2005, *Science*, 307, 1288
- Holman, M. J. & Wiegert, P. A., 1999, *AJ*, 117, 621.
- Kipping, D.M., 2009a, *MNRAS*, 392, 181
- Kipping, D. M., 2009b, *MNRAS*, 396, 1797
- Koch, D. G., et al. 2004, *Proc. SPIE*, 5487, 1491
- Lega E. & Froeschlé, C., 2001, *CeMDA*, 81, 129
- Lichtenegger, H. 1984, *CeMDA*, 34, 357.
- Mathieu, R.D., 1994, *ARA&A*, 32, 465
- Mathieu, R. D., Ghez, A. M., Jensen, E. L. N. & Simon, M., 2000, in *Protostars and Planets IV*, ed. V. Mannings, A. P. Boss, and S.S. Russell (Tucson: Univ. Arizona Press), pp.703
- Miralda-Escudé, J. & Adams, F.C. 2005, *Icarus*, 178, 517
- Muterspaugh, M. W., Konacki, M., Lane, B. F., & Pfahl, E. 2010, in "Planets in Binary Star Systems", N. Haghighipour (ed.), *Astrophysics and Space Science Library*, Vol. 366. Berlin: Springer, ISBN: 978-90-481-8686-0, p.77-103
- Muterspaugh, M. W., Lane, B. F., Kulkarni, S. R., Konacki, M., Burke, B. F., Colavita, M. M., Shao, M., Hartkopf, W. I., Boss, A. P., & Williamson, M., 2010, *MNRAS*, 140, 1657
- Pilat-Lohinger, E. & Dvorak, R., 2002, *CeMDA*, 82, 143.
- Pilat-Lohinger, E., Funk, B., Dvorak, R., 2003, *A&A*, 400, 1085.
- Queloz, D., Mayor, M., Weber, L., Blécha, A., Burnet, M., Confino, B., Naef, D., Pepe, F., Santos, N., & Udry, S., 2000, *A&A*, 354, 99
- Raghavan, D., Henry, T.J., Mason, B. D., Subasavage, J.P., Jao, W.-C., Beaulieu, T. D., & Hambly, N. C., 2006, *ApJ*, 646, 523
- Rodriguez, L. F., D'Alessio, P., Wilner, D. J., Ho, P. T. P., Torrelles, J. M., Curiel, S., Gomez, Y., Lizano, S., Pedlar, A., Canto, J. & Raga, A.C., 1998, *Nature*, 395, 355
- Schneider, J. & Chevreton, M. 1990, *A & A*, 232, 251.
- Schneider, J. & Doyle L.R., 1995, *EM&P*, 71, 153.
- Silbert, J., Gledhill, T., Duchene, G. & M'enard, F., 2000, *ApJL*, 536, L89
- Steffen, J. H., & Agol, E. 2005, *MNRAS*, 364, L96
- Sybilsky, P., Konacki and Kozłowski, S., 2010, *MNRAS*, 405, 657.
- Trilling, D. E., Stansberry, J. A., Stapelfeldt, K. R., Rieke, G. H., Su, K. Y. L., Gray, R. O., Corbally, C. J., Bryden, G., Chen, C. H., Boden, A. & Beichman, C. A., *ApJ*, 658, 1264
- White R. J., Ghez A. M., Reid I. N. & Schultz G., 1999, *ApJ*, 520, 811
- Zucker, S., Mazeh, T., Santos, N.C., Udry, S., Mayor, M., 2004, *A & A*, 426, 695.
- Zahn, J.-P. & Bouchet, L. 1989, *A&A*, 223, 112